11th International Symposium on Magnetic Bearings
August 26-29, Nara, Japan

MODEL-FREE CONTROL METHODS FOR RECOVERY FROM TOUCHDOWNS INVOLVING CIRCULAR WHIRL

Matthew O T Cole
Dept. of Mechanical Engineering, Chiang Mai University, Chiangmai 50200, Thailand
motcole@chiangmai.ac.th

ABSTRACT
In this paper, the dynamics associated with rotor-stator touchdowns involving full circular rub are considered. The expected range of phase shifts occurring in various measurable signals are examined from a theoretical standpoint, with the aim of developing model-free control algorithms that can recover contact-free rotor levitation from a state involving persistent rub with touchdown bearings. Two different strategies are proposed, according to whether touchdowns planes can be considered collocated with the AMBs or not. Requirements for successful operation, in terms of available sub-models and measurement information, as well as possible deficiencies are explained and verified through experimental tests on a multi-mode flexible rotor test rig.

INTRODUCTION
The theoretical problem of coupled rotor-stator whirl involving contact was first considered for multi-mode systems by Black [1], who assumed steady circular whirl in a system with radially isotropic characteristics. This type of analysis, which will be adapted for the purposes of this paper, is also applicable to auxiliary bearing touchdowns when caused by excessive synchronous disturbances rather than control system faults. Black's approach of considering circular orbit solutions to the equations of motion has been employed by a number of researchers with the view to improving the design of mechanical components in auxiliary bearing systems [2-5]. When friction is included, the method is also applicable to backward whirl response prediction and has been widely considered as a means of predicting when systems are prone to backward whirl [6-8]. To this author's knowledge, Black's analysis of forward whirl rub behaviour has not previously been exploited in any direct way for the purpose of active controller design.

SYNCHRONOUS WHIRL EQUATIONS
The geometry associated with touchdown is shown in Figure 1. The surround is assumed to have uniform radial clearance c when the rotor and stator centres are at the static equilibrium position O. The deflection of the rotor $\mathbf{z}_r$ may result from rotor unbalance in addition to the action of the contact force $\boldsymbol{f}$. The deflection of the surround $\mathbf{z}_s$, results solely from contact with the rotor. Assuming circular whirl of the rotor and surround occurs, complex notation may be adopted:

$$\mathbf{z}_s = x_s + \mathrm{j}y_s = Z_s \mathrm{e}^{\mathrm{j}\Omega t}, \quad \mathbf{z}_r = x_r + \mathrm{j}y_r = Z_r \mathrm{e}^{\mathrm{j}\Omega t},$$
$$\boldsymbol{f} = f_x + \mathrm{j}f_y = F\mathrm{e}^{\mathrm{j}\Omega t} \tag{1}$$

Linear dynamics of the rotor and stator vibration imply that the complex amplitudes are related by [1]:

$$Z_r = Q + A_f(\Omega)F \tag{2}$$
$$Z_s = -B_f(\Omega)F \tag{3}$$

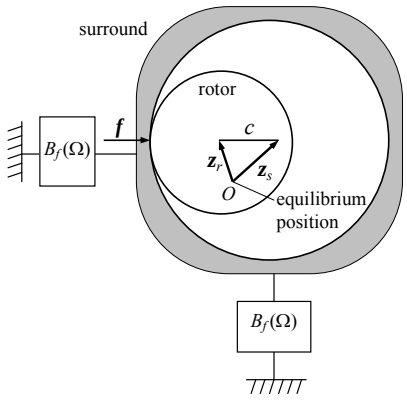

FIGURE 1: Touchdown of a rotor with a circular surround

The complex amplitude Q is the vibration of the rotor due to unbalance that would have occurred without contact. The parameters A_f and B_f, sometimes termed polar receptances or influence coefficients, are the complex values of the frequency response functions relating displacements in the contact plane to the contact force. Taking the contact normal as the zero phase reference, so that $F = f\mathrm{e}^{\mathrm{j}\phi}$, where f is the contact force magnitude (hence real valued) and ϕ is the friction angle, it then follows that

$$Z_s - Z_r = c \tag{4}$$

And so from (2) and (3)

$$Q + (A_f + B_f) f\mathrm{e}^{\mathrm{j}\phi} + c = 0 \tag{5}$$

This vector equation relates the non-contact rotor response Q to the corresponding response involving circular rub with contact force magnitude f. Solution pairs Q and f are related by the geometry shown in figure 2.

Writing $(A_f + B_f)\mathrm{e}^{\mathrm{j}\phi} = r\mathrm{e}^{\mathrm{j}\alpha}$, it follows that, for a given non contact orbit magnitude $|Q|$, the corresponding contact force f is the solution to the quadratic equation

$$r^2 f^2 + \cos\alpha\, crf + c^2 - |Q|^2 = 0 \tag{6}$$

If the magnitude of Q is greater than c then vibration without contact is impossible. There can then only be one solution for f that is positive and therefore physically plausible. An example of such a case is indicated by Q and f in Figure 2. However, at running speeds for which $-270^\circ - \phi < \angle A_f + B_f < -90^\circ - \phi$ (i.e. $\cos\alpha < 0$), certain unbalance levels can cause a response involving persistent contact to occur even when the normal operating orbits are within the clearance limit. Such situations tend to occur when running above the critical speed for coupled rotor-stator vibration, when the phase of $A_f + B_f$ is less than -90°. Note that there are then two positive solution for f for any given $|Q| < c$, although the solution having a lower value of f corresponds to an unstable orbit. A full investigation of the response behaviour associated with eqns (2-5) is given by Black [1], who deals with various examples involving multimode rotor and stator dynamic models. Although the analysis presented by Black considers only the case of a single contact, the results obtained are important for rotor-magnetic bearing systems as they explore the conditions under which jumps from contact-free to continuous rub conditions may occur.

CONTROL IMPLICATIONS

The equations (2-6) can also give useful insight on the potential difficulties of recovering contact-free conditions when persistent coupled vibration of the rotor and stator has been instigated. In passive rotor systems the only possible course of action is a rotor rundown. The risk associated with such a procedure is that a rundown would likely require transition through a critical speed for coupled rotor-stator vibration that would increase the severity of vibration and potentially lead to machine damage, although auxiliary bearing systems are usually designed with this in mind. Significantly, in magnetic bearing systems there is the possibility of using appropriate control forces applied by the bearings to recover contact-free conditions without the need for rundown.

Consider a synchronous rotating control force applied through a magnetic bearing $u = U\mathrm{e}^{\mathrm{j}\Omega t}$. The contact-free orbit in the touchdown plane is then given by

$$Q = Q_0 + A_u U \tag{7}$$

Here, Q_0 is the response without control and A_u is the influence coefficient relating bearing forces to the displacement in the touchdown plane. If contact has occurred then the contact-free orbit Q will not be measurable. Nonetheless recovering contact-free conditions will require a reduction in the magnitude of Q, which will then produce a corresponding reduction in f and Z_r. If Q_0 and A_u are both known, the required control action can be calculated according to

$$U = -A_u^{-1} Q_0 \tag{8}$$

However, if the contact-free orbits Q_0 have not been determined, or if the rotor unbalance condition could have changed, then an alternative procedure must be used.

Previously, a number of unbalance control schemes have been proposed for magnetic bearings in which the controller acts on measurements of rotor displacements and produces synchronous control forces at the bearings, updated in an iterative manner to cancel the effects of unbalance forces e.g. [9-13]. Although conditions involving stator contact are not considered in these studies, a similar approach will be used here. For a single measurement plane and control force plane the control law may take the form

$$U_{k+1} = U_k + \Gamma Z_{rk} \tag{9}$$

Where Γ is a complex gain of sufficiently small magnitude. From (7), the updated orbit is then given by

$$Q_{k+1} = Q_k + \Gamma A_u Z_{rk} \tag{10}$$

Consider the vector geometry associated with eqns (2-6), as shown in Figure 2. From triangle OAB, the phase difference between Z_r and Q varies with contact force magnitude f, but never by more than 180° for a fixed running speed (i.e. fixed values of A_f and B_f). It is therefore always possible to determine a complex value of $\Gamma = \delta\,\mathrm{e}^{\mathrm{j}\alpha}$ such that $-\angle Q - 90^\circ < \alpha + \angle A_u Z_r < -\angle Q + 90^\circ$. Which from (10) then implies that $|Q_{k+1}| < |Q_k|$ for sufficiently small δ. Therefore, after applying a number of control updates the rotor orbits

will be sufficiently small that contact with the surround will cease. The difficulties associated with such a scheme are that:

1. the appropriate value of Γ varies with running speed and so a controller that works at one speed may be unstable at other speeds.

2. the influence coefficient/s A_u and the expected range of phase shifts under contact must be determined for each possible running speed.

3. the control scheme takes no account of the severity of contact or whether contact has even occurred.

Multi-input multi-output versions of this type of scheme have also been proposed and shown to be effective on flexible rotor AMB systems [5,14]. However, further identification routines were used to exactly quantify the expected levels of phase shift under contact and thereby ensure stable operation.

MODEL-FREE CONTROL APPROACHES

In this paper we will consider that the rotor-stator system possesses the characteristics of a passive mechanical structure and therefore the complex coefficients A_f and B_f have phases within the range (-180°, 0). The implications of this for expected phase shifts in some measurable signals are embodied in the following two conditions:

Condition 1

With reference to Figure 3, the condition $\angle(A_f + B_f) \in (-180^\circ, 0^\circ)$ implies that the point A can never be below the line MM' that passes through the point $-c$ and is parallel to the contact force vector. The phase of Q relative to the contact force is therefore always in the range (0°, 180°), irrespective of running speed:

$$\angle Q - 180^\circ < \angle F < \angle Q \tag{11}$$

Condition 2

Again referring to Figure 3, the condition $\angle A_f \in (-180^\circ, 0^\circ)$ implies that the point A can never be below the line NN' passing through B parallel to the contact force vector. With some consideration, it should be clear that this condition implies that $\angle Q - \angle A_f > \angle Z_r$ and also that $\angle Q - \angle A_f < \angle Z_r + 180^\circ$. Consequently,

$$\angle Q - 180^\circ < \angle A_f + \angle Z_r < \angle Q \tag{12}$$

Note that for a given running speed (fixed value of A_f) condition 2 also implies that the phase of Q and Z_r can never vary by more that 180 degrees, as has been previously indicated.

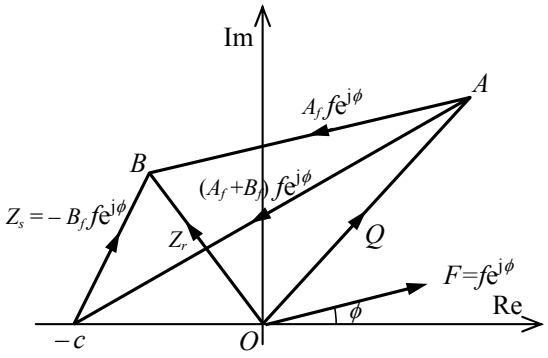

FIGURE 2: Geometry of rotating frame vectors associated with rotor-stator interaction involving synchronous whirl

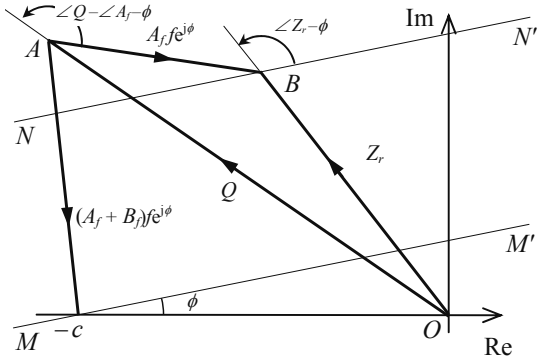

FIGURE 3: Points A and B are confined to upper regions of the complex plane owing to passive dynamics

CASE A: Collocated AMBs and touchdown planes

Suppose that a magnetic bearing and contact plane are sufficiently well collocated so that $A_f = A_u$. In such cases we may again consider the control law

$$U_{k+1} = U_k + \delta e^{j\alpha} Z_{rk} \tag{13}$$

Selecting the controller phase shift as $-\pi/2$ implies

$$Q_{k+1} = Q_k + \delta e^{-j\pi/2} A_f Z_{rk} \tag{14}$$

From condition 2 it then follows that $|Q_{k+1}| < |Q_k|$, at least for sufficiently small scalar $\delta > 0$. The control algorithm (13) is appropriate to systems with collocated magnetic bearings and touchdown bearings, and requires no knowledge of A_f or A_u. The controller will act to reduce the orbit sizes irrespective of whether contact has occurred or not. In many cases the collocation requirement could be relaxed providing that running speeds are sufficiently low that phase differences between A_f and A_u, as would typically arise from high order flexural modes, are negligible. Note however that to adopt this algorithm the absolute motion of the rotor must be measurable and so it is not appropriate to cases where rotor displacement

measurements are affected by motion of the stator. Of course the assumption of steady-state conditions used in deriving the expected phase shifts is not always realistic, but providing there are only slow changes in control forces, the model is usually valid.

In some applications, it may be advantageous to use a control algorithm that acts only to eliminate contact or rub once it has been instigated. A variation of the proposed control approach could be applied when the stator can be represented by a simple compliance model (possibly nonlinear) of the form $Z_s = -k_s F$. In such cases the Z_s, Z_r and F are geometrically related as illustrated in Figure 4. The possibility considered now is that motion of the stator in the contact plane or the contact force can be measured (being loosely equivalent as they have equal and opposite phase). In this case, the stator motion has a phase advance over the rotor motion which for small deflections is equal to the friction angle ϕ. This phase advance drops to zero as the displacements become large compared with the clearance. Here the control law may take the form

$$U_{k+1} = U_k + \delta\, \mathrm{e}^{\mathrm{j}\alpha} Z_{sk}\,,\ \alpha = -\pi/2 - \phi \qquad (15)$$

Or alternatively, with use of contact force measurements,

$$U_{k+1} = U_k + \delta\, \mathrm{e}^{\mathrm{j}\alpha} F_k\,,\ \alpha = \pi/2 - \phi \qquad (16)$$

A potential shortfall of this algorithm is that an estimate of the friction angle ϕ is required for implementation and if this friction angle varies too much with operating speed then it will not be possible to achieve stable control over the entire range of running speeds with a single gain value. Some fairly simple scheduling of gain values could however be adopted.

CASE B: Non-collocated AMBs and touchdown planes

When non-collocation is a significant factor in as much as the phase of A_f and A_u deviate, then it would seem that a controller that exploits condition 1 may be a better option. However, knowledge of A_u is then inevitably required, this can be easily obtained through identification routines that apply test forces at the bearing. In this case the control law can be taken as

$$U_{k+1} = U_k + \delta\, \mathrm{e}^{\mathrm{j}\alpha} F_k\,,\ \alpha = -\angle A_u - \pi/2 \qquad (17)$$

$$Q_{k+1} = Q_k + \delta \left| A_u \right| e^{-j\pi/2} F_k \qquad (18)$$

Which, from condition 1, implies that $\left|Q_{k+1}\right| < \left|Q_k\right|$ for sufficiently small δ. Alternatively, when $Z_s = -k_s F$ then selecting

$$U_{k+1} = U_k + \delta\, \mathrm{e}^{\mathrm{j}\alpha} Z_{sk}\,,\ \alpha = -\angle A_u + \pi/2 \qquad (19)$$

leads to the same conclusion.

The contact control approach is shown schematically in Figure 5 with alternatives of feedback of contact force or stator displacement measurements. In practice both the gain δ and phase shift α used in the control feedback would be selected according to choice of measurement signal and scheduled with running speed when necessary. It should be remarked that direct measurement of stator deflection or contact forces can also be used for other tasks that might enhance the 'smart machine' capabilities of a magnetic bearing system as such measurements can be used for monitoring and assessing touchdown events, condition monitoring of touchdown bearings as well as for purposes of control.

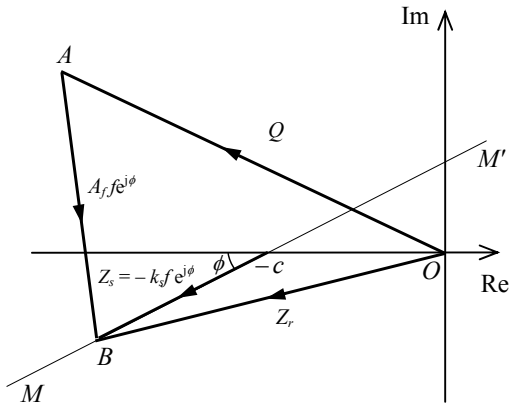

FIGURE 4: Point *B* falls on the line *MM′* when the stator is modeled as a compliant surround.

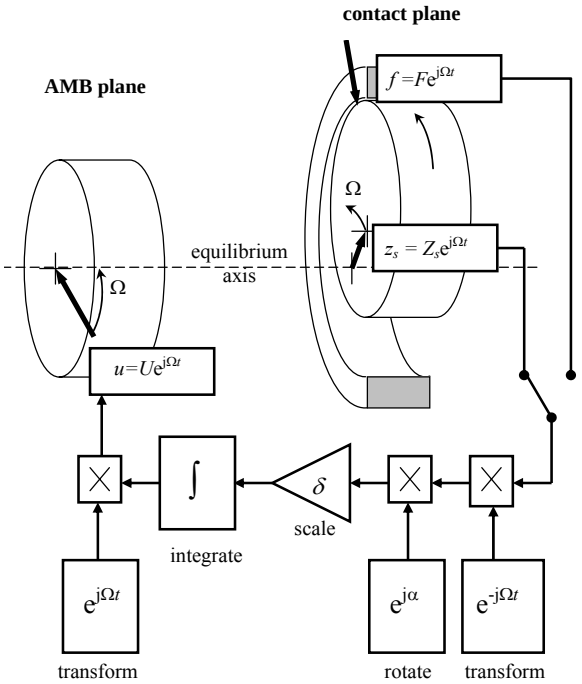

FIGURE 5: Schematic of contact control approach

EXPERIMENTAL TESTS

To verify whether the operating principles of the proposed control strategies are effective on a real system, a 2-disk flexible rotor-stator interaction test rig with a single AMB has been used for testing. In this system (Figure 6), the magnetic bearing and contact plane are not collocated: this allows the associated difficulties for control to be explored fully.

The rotor shaft has diameter 10 mm and is supported by two ball bearings at each end giving a span of 700 mm. The AMB core (disk 1) and the contact disk (disk 2) are spaced approximately equidistantly on the shaft. The stator contact mechanism (Figure 7) consists of a circular surround of mass 0.55 kg supported by four transverse rods of variable length that allow lateral stiffness to be selected freely. The inner diameter of the surround is 64 mm and the nominal radial clearance is 400 μm. During all tests, the contact surfaces were lubricated with light oil.

PID control of the AMB is used to provide stable centring of the rotor and also increases modal damping. For most purposes, the rotor can be considered as a 'two-mass' system with the first two natural frequencies for rotor vibration (20 Hz and 70 Hz) both being within the nominal running speed range of 0 – 100 Hz. The full frequency response data for additional control force inputs applied at the bearing is shown in Figure 8. In terms of phase response, disk 1 and disk 2 can be considered collocated up to frequencies of 40 Hz.

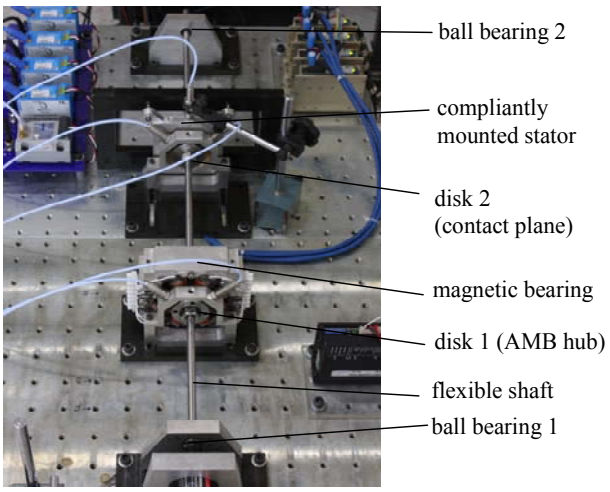

FIGURE 6: Flexible rotor-stator interaction test rig

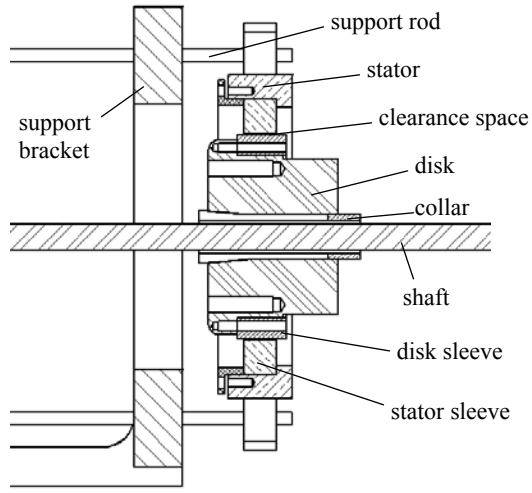

FIGURE 7: Stator-disk contact mechanism

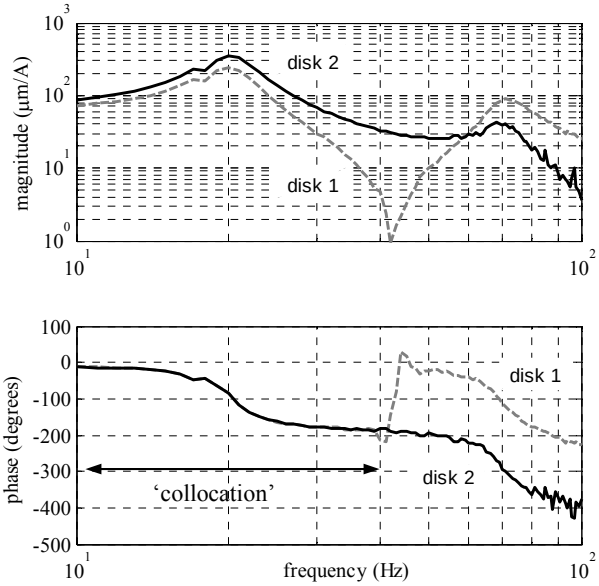

FIGURE 8: Frequency response from AMB control current to rotor displacement in contact plane (disk 2) and AMB plane (disk 1)

The rotor was set with moderate levels of unbalance, resulting in the run-up response shown in Figure 9. During these 'low speed' tests the stator support was set with stiffness 0.42 MN/m, giving the stator a 'sprung mass' behaviour with natural frequency of approximately 140 Hz. Figure 9 compares the response magnitude, with and without the stator mechanism fitted. During run-up with the stator fitted, contact commences at approximately 10 Hz. Contact is at first intermittent, due to slight misalignment of the rotor and surround, but becomes continuous at speeds higher than 15 Hz. Although the magnitude of rotor vibration grows only slightly as the speed increases further, the stator

vibration increases markedly until at a speed of 24 Hz the rotor falls out of contact. Deflection of the stator was monitored by a high precision non-contact probe (Bently Nevada 3300 REBAM) and reached a maximum amplitude of 6 μm as seen in Figure 9. It should be noted that the results presented here show only synchronous components of the vibration and that other vibration components can and do occur, particularly when contact with the stator is intermittent. Of course, these vibration components are not evident in the (time-averaged) estimate of the synchronous component and will not be acted on by the controller.

The run-up was repeated with the contact control algorithm (15) operating. The controller was configured to only update the control force when the stator vibration exceeded 1 μm in magnitude. This was so that the controller did not act on measurements of low level vibration transmitted through the foundation structure. The response of the controlled system (Figure 9) is similar to the uncontrolled case up to 15 Hz. However, above this rotational frequency, the control action updates the control force to maintain the magnitude of steady state stator vibration below 1μm. Superimposed on the figure are the boundaries for intermittent contact and continuous contact, applicable when circular orbits occur. The model-free control works well in low speed tests where the running speed is kept below 40 Hz, but it should be made clear that this success relies on the fact that

1) the 'collocation' assumption is valid for $\Omega < 40$ Hz

2) the compliant stator model is valid for $\Omega << 140$ Hz

Of course, the first assumption breaks down for higher running speeds and this controller was found to become unstable if rub occurs while passing through the second critical speed.

To achieve contact control at higher rotational frequencies the non-collocation must be accounted for, as with the control law (19). With this controller, the scheduling of the controller phase shift according to $\alpha = -\angle A_u + \pi/2$ was based on $\angle A_u$ calculated from the frequency response data of Figure 8 and implemented using a look-up table approach. The results are shown in Figure 11. It can be seen that, as the system passes through the first critical speed, the controller adapts the control force so that only light contact with the stator occurs. Again the stator vibration is kept below 1μm in magnitude. As the rotor speed approaches the second critical speed, contact recommences at around 60 Hz. At first the controller appears to respond successfully, as the synchronous vibration components of both the rotor and stator vibration are reduced. However this does not give the complete picture, as the orbital motion of the rotor and stator is not circular and so intermittent contact with the surround still occurs. Above the critical speed the controller is unable to maintain light contact. At this time the stator undergoes severe aperiodic vibrations and the control cannot be considered stable. The poor result with this controller was attributed to the failure to maintain steady circular whirl vibration conditions, rather than a flaw in the working principles of the control algorithm.

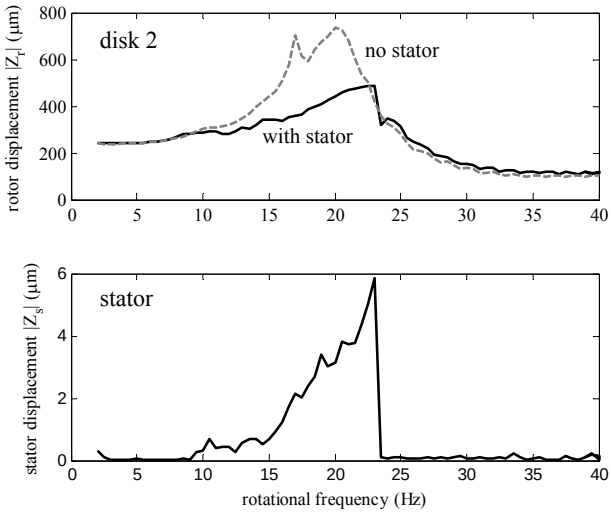

FIGURE 9: Unbalance response at disk 2 with and without stator contact interaction (PID feedback control only)

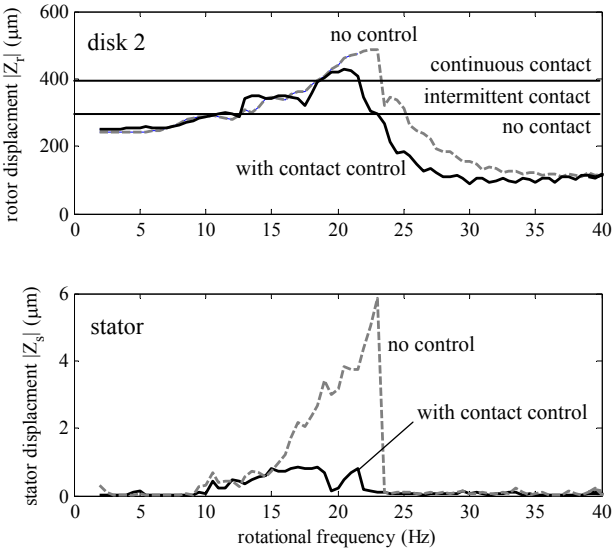

FIGURE 10: Unbalance response with and without feedback of stator deflection measurements (control with equation (15))

The occurrence of intermittent contact and non-circular responses can be partly attributed to the dynamic behaviour of the stator mechanism, as the natural frequency for lateral vibration of the structure was only slightly higher than the maximum rotational frequency and has only light damping ($\zeta < 0.1$). In an effort to reduce the dynamic influence of the stator, the stator support stiffness was increased to 1.0 MN/m, thus increasing the stator natural frequency to 215 Hz. Repeating the run-up test in this case gave much better results, as can be seen from Figure 12. The rotor passes through the second critical speed with the synchronous component of the stator vibration maintained close to the set limit of 1 μm. The synchronous component of the rotor vibration is also constrained quite effectively. Although these results appear much improved, and stability of the control is maintained, intervals of aperiodic vibration were still found to occur around the second critical speed. These caused jumps in the time-averaged measurements when the synchronous components of vibration were fluctuating significantly. The time-averaged values were however regulated quite effectively.

CONCLUSIONS

This paper has proposed the use of a geometric analysis of circular whirl with rub as a basis for model-free controller design for robust synchronous control. The analysis shows that measurements of contact force or stator displacements can be usefully employed to limit contact forces during rub conditions. The need for models of the system dynamic compliance in the contact plane can be circumvented if the stator and rotor structures behave like passive structures. In experimental tests, controller stability problems were found to arise when aperiodic and non-circular orbits occurred. This problem appears to be avoidable if damping levels for stator vibration modes are sufficiently high, or if stator modes have natural frequencies that are sufficiently well separated from the synchronous frequency.

In some situations, improved versions of these algorithms could be developed that are based on speed-scheduling of gains. This need not require full or accurate system models but rather approximate knowledge of rotor critical speeds where phase swings tend to occur and could usefully be accounted for in the control action. Although two basic approaches have been outlined in this paper it is not presupposed that these would suit all types of system. However, it is also quite possible that other sufficiently bounded phase relations can be determined that can also be exploited for the purposes of control.

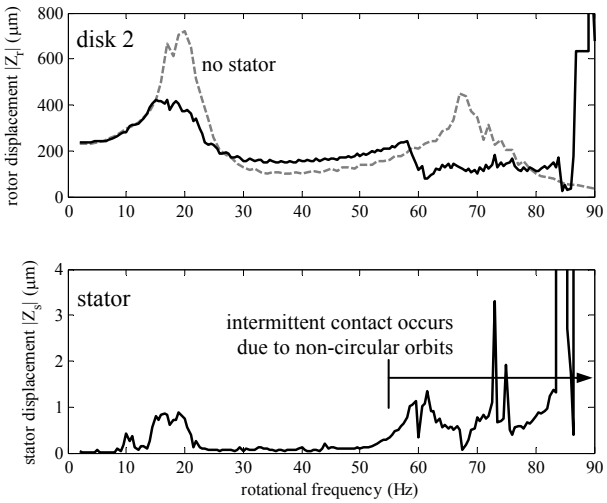

FIGURE 11: Unbalance response with feedback of stator deflection measurements (control with equation (19)). Stator with 'low' natural frequency (140 Hz)

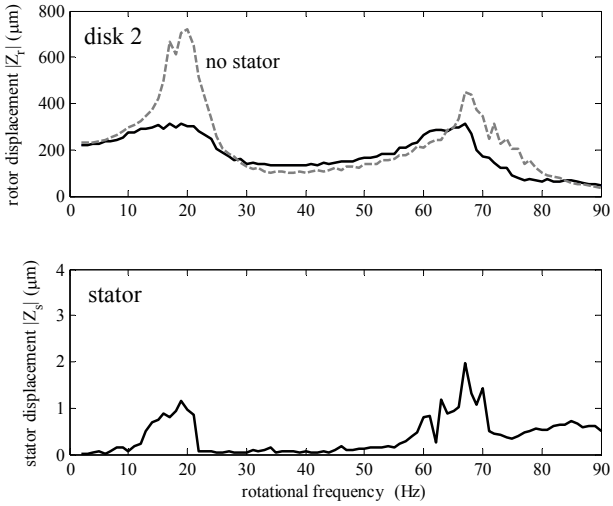

FIGURE 12: Unbalance response with feedback of stator deflection measurements (control with equation (19)). Stator with 'high' natural frequency (215 Hz)

REFERENCES

1. Black, H. F. Interaction of a whirling rotor with a vibrating stator across a clearance annulus. *J. Mech. Eng. Sci.*, 1968, **10**(1), 1–12.

2. Lawen, J. L. & Flowers, G. T. Interaction dynamics between a flexible rotor and an auxiliary clearance bearing. *J. Vib. Acoust.*, 1999, **121**, 183–189.

3. Xie, H., Flowers, G. T., Feng, L. and Lawrence, C. Steady-state dynamic behavior of a flexible rotor with auxiliary support from a clearance bearing. *ASME J. Vib. Acoust.*, 1999, **121**, 78-83.

4. Fumagalli, M, Schweitzer, G Motion of a rotor in retainer bearings. In *Proc. 5th Int. Symp. Magnetic Bearings,* Urawa, Japan, August 1996, pp. 509-514.

5. Keogh, P. S. & Cole, M. O. T. Rotor vibration with auxiliary bearing contact in magnetic bearing systems, Parts 1 and 2. *J. Mech. Eng. Sci.*, 2003, **217**(4), 377–392.

6. Bartha, A. R. Dry friction backward whirl of rotors. Doctoral dissertation ETH No. 13817, ETH, Zurich, 2000.

7. Childs, D. W. & Bhattacharya, A. Prediction of dry-friction whirl and whip between a rotor and a stator. *J. Vib. Acoust.*, 2007, **129**(3), 355–362.

8. Cole, M. O. T. On frequency response based prediction of rotor-stator circular rub behaviour. In *Proc. 11th Int. Conf. on Vibration in Rotating Machinery,* Exeter, UK, 8-10, September, 2008, paper C663.

9. Burrows, C.R. and Sahinkaya, M.N., Vibration control of multi-mode rotor bearing system. *Proc. Roy. Soc. Lond.,* Series A, 1983, **386**, 77-94.

10. Keogh, P.S., Burrows, C.R., and Berry, T., On-line controller implementation for attenuation of synchronous and transient rotor vibration. *ASME Journal of Dynamic Systems, Measurement, and Control*, 1996, **118**, 315-321.

11. Manchala, D. W., Palazzolo, A.B., Lin, Kasak, A.K., Montague, J. and Brown, G.V., Constrained quadratic programming active control of rotating mass imbalance. *Journal of Sound and Vibration*, 1997, **205**, 561-580.

12. Knospe, C., Hope, R., Fedigan, S., and Williams, R., Experiments in the control of unbalanced response using magnetic bearings. *Mechatronics*, 1995, **5**, 385-400.

13. Nonami, K. and Liu, Z., Adaptive unbalance vibration control of magnetic bearing system using frequency estimation for multiple periodic disturbances with noise. *IEEE Conference on Control Applications - Proceedings,* v 1, Kohala Coast, HI, 1999, 576-581.

14. Keogh, P.S., Cole, M.O.T., Sahinkaya, M.N. & Burrows, C.R. On the control of synchronous vibration in rotor/magnetic bearing systems involving auxiliary bearing contact,' *ASME J. Eng. Gas Turbines and Power,* 2004, **126**, April, pp. 366-372.